Second Harmonic Generation from Aluminum Plasmonic Nanocavities: from Scanning to Imaging

Tchiya Zar,[1] Alon Krause, Omer Shavit,[1,2], Hannah Aharon,[1] Racheli Ron,[1] Martin Oheim,[2] and Adi Salomon[1,2]

[1]Department of Chemistry, BINA Nano Center for advanced materials, Bar-Ilan University, Ramat-Gan, Israel.

[2]Université de Paris, SPPIN - Saints-Pères Paris Institute for the Neurosciences, CNRS, Paris F-75006, France.

Supporting Information

Figures for additional information:

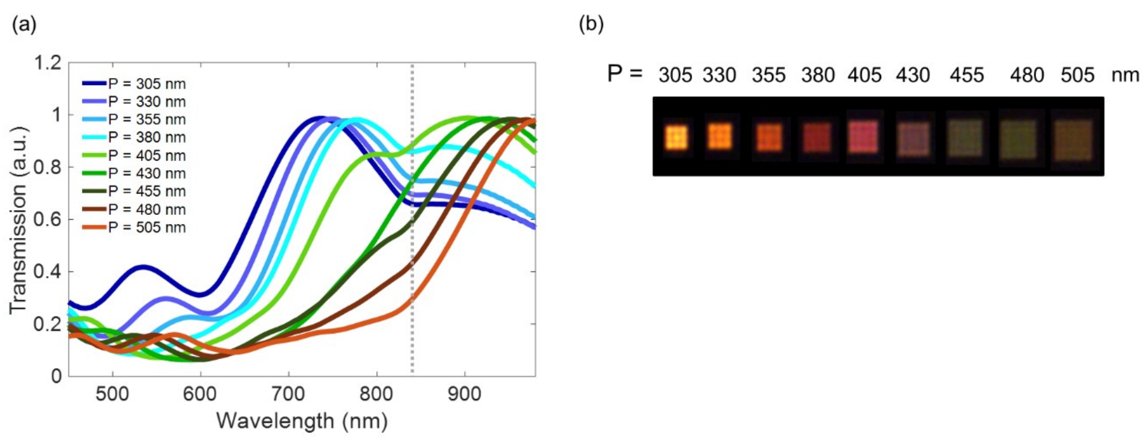

Figure S1: Optical transmission microscopy spectra and transmission microscope images of triangular hole-arrays. (a) Transmission spectra of the triangles hole arrays, the dispersion is well notable. Gray dashed line indicate the transition band in aluminum. (b) Light microscope images of the structures with the different periodicities (*P*, (nm)) as indicated.

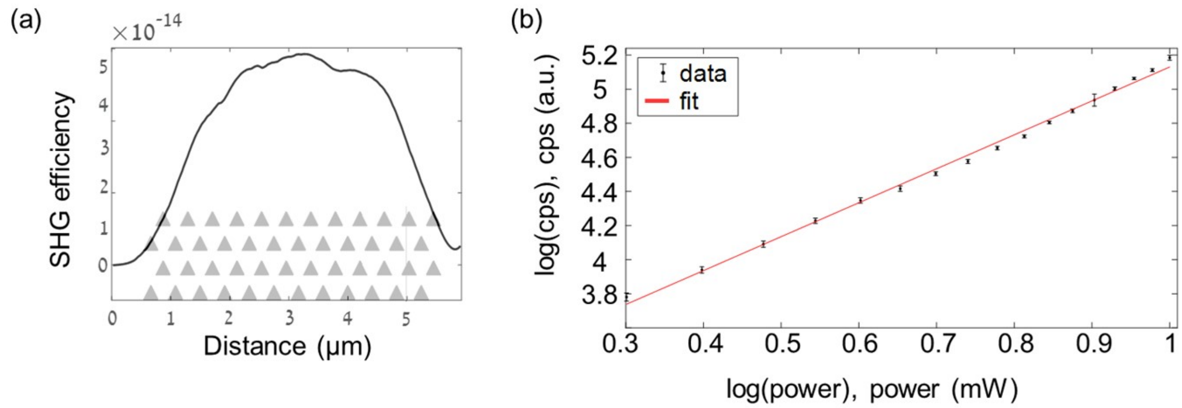

Figure S2: (a) Cross section of the SHG response along triangular hole-array with P = 380 nm (figure 2b in the main text). The triangles array inset added to show the borders of the array compared to the response intensity. Scale is normalized according to conversion efficiency. (b) Log-log plot of SHG power versus excitation power from a triangle array, P = 405 nm; the slope is ≈ 2, with R^2=0.996. The black dots are the experimental data, and the red line is the linear fit.

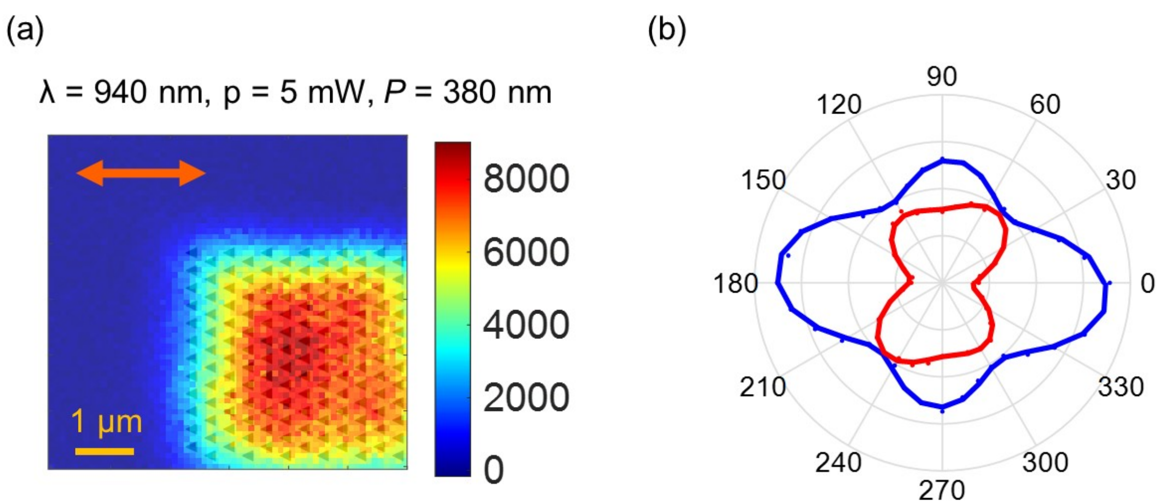

Figure S3: (a) SHG response of triangular hole-array with P = 380 nm over scan area of $6 \times 6\mu m^2$, λ = 940 nm, p = 5 mW. (b) Polar plots of the polarization dependent SHG response of the array. Those measurements have been taken more than three years after the measurements presented in the main text under the same conditions (figures 2b, 4b).

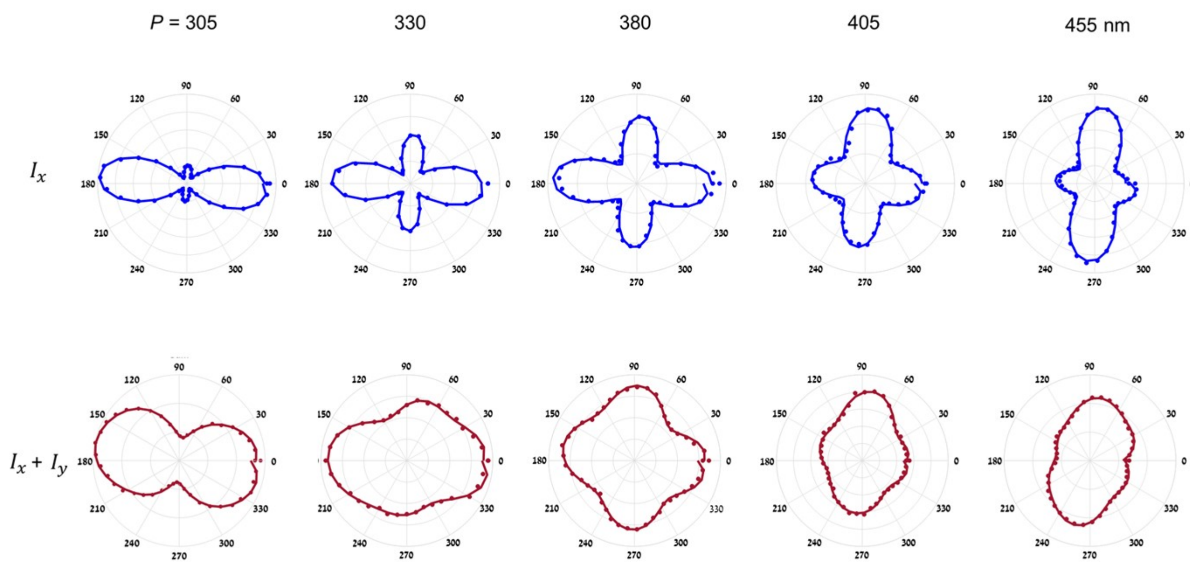

Figure S4: Rotational SHG measurements taken form the set of hole-array (aluminum) with periodicities *Ps* of 305, 330, 380, 405 and 455 nm as shown. λ = 940 nm, p = 5 mW.

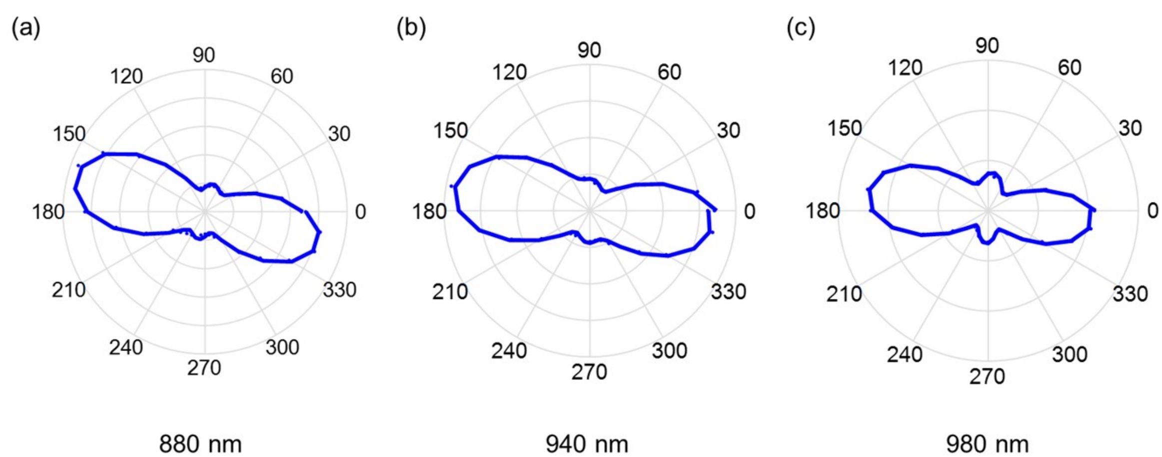

Figure S5: Rotational SHG for triangular hole array, *P* = 305 nm, under three different laser illumination wavelengths of (a) 880, (b) 940, and (c) 980 nm, showing no significant difference of the emission pattern. The responses were collected by one channel (I_x).

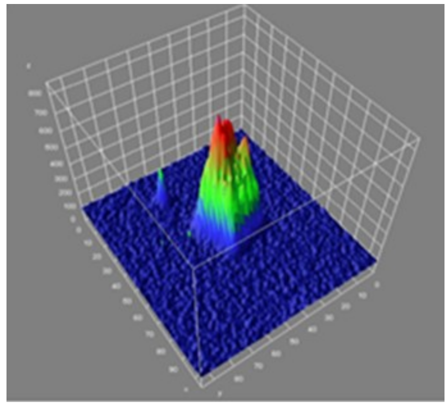

Figure S6: more information about the OASIS.

Experimental section:

As discussed in the main text, the samples prepared on cleaned glass substrate, and cover with thin metal film by deposition. Figure S7 shows illustration of the sample after fabrication by focus ion beam (FIB) and cover by layer of PVA (~ 150 nm).

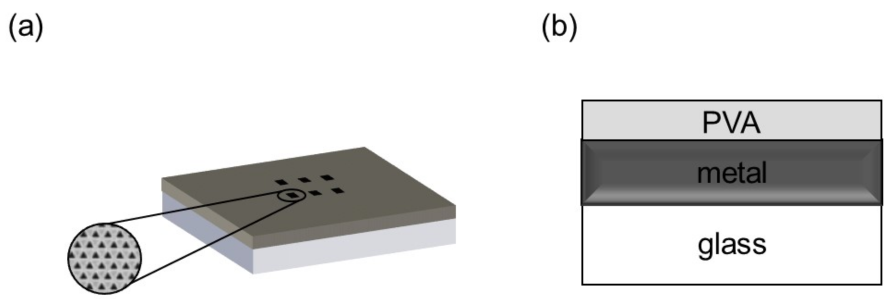

Figure S7: Description of the sample. The structures are milled in 200 nm Al film evaporated on SiO_2 substrate (glass). (a) Schematic description of the glass coated with ~ 200 nm of metal. The arrays were fabricated by FIB technique in the center of the sample. (b) Schematic cross-section description of the glass coated with 200 nm metal and a ~ 150 nm PVA polymer layer, coated by a spin coater technique.

Full description of the second harmonic generation set-up, shows in figure 2a at the main text:

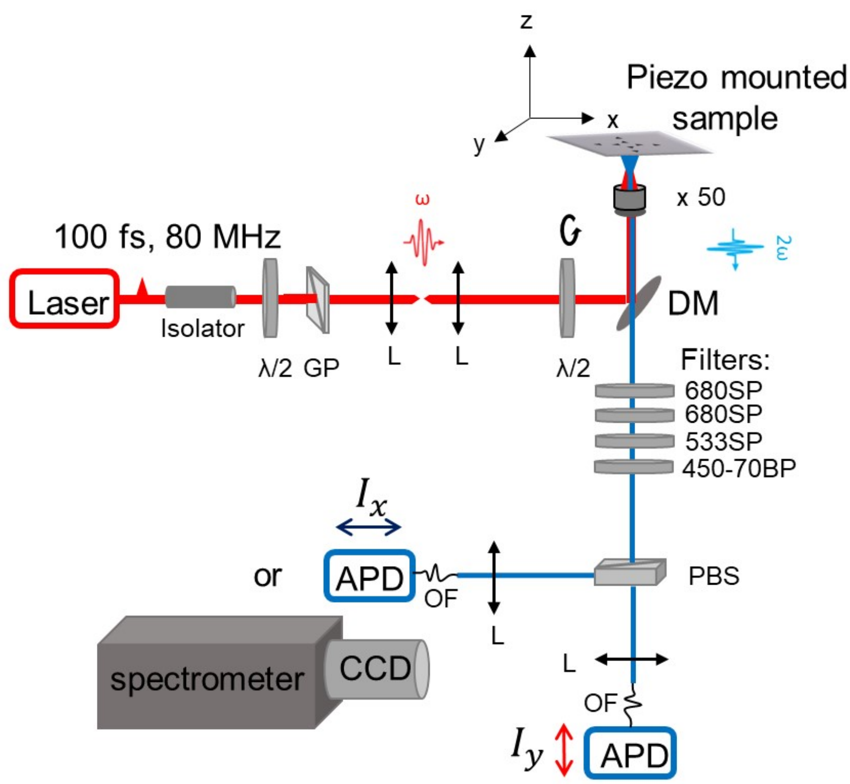

Figure S8: Schematic illustration of the SHG imaging setup and optical path: Isolator – optical Faraday cage isolator, λ/2 – half wave plate, GP – Glan-Taylor polarized beam splitter, L – lens, DM – dichroic mirror, SP – short-pass filters, BP – band-pass filter, PBS – polarizing beam splitter, APD – avalanched photodiode, Spectrometer– computerized double slit mounted spectrometer, OF – optical fiber, CCD – an electro magnetic charge-coupled device (EMCCD) detector. The circularly oriented arrow corresponds to the motorized rotation stage. There are four BPFs in the series presented with a total optical density (OD) of 42.25.

Intensity and second harmonic efficiency section:

Since the SH process has low efficiency, and the optical system weakens the response, to know how effective these arrays are, we will consider the efficiency of the SHG process.

Example of calculation:

Count rate measured by both APDs from array with periodicity of 405 nm was ~27000 counts per second (cps), for the in-axis polarization state of a fundamental field. The APD's dark noise is about ~ 200 cps, neglected for plasmonic structures' response but not for surface' response.

To estimate the total optical efficiency, we considered the transmittance efficiency of all the relevant components in our experimental setup for series of wavelengths. The total transmittance efficiency of the system at 470 nm is $t_e \sim 13\%$, which gives a corrected measurement rate of $2.05 \cdot 10^5$ cps for the in-axis polarization state for the $P = 405$ nm array.

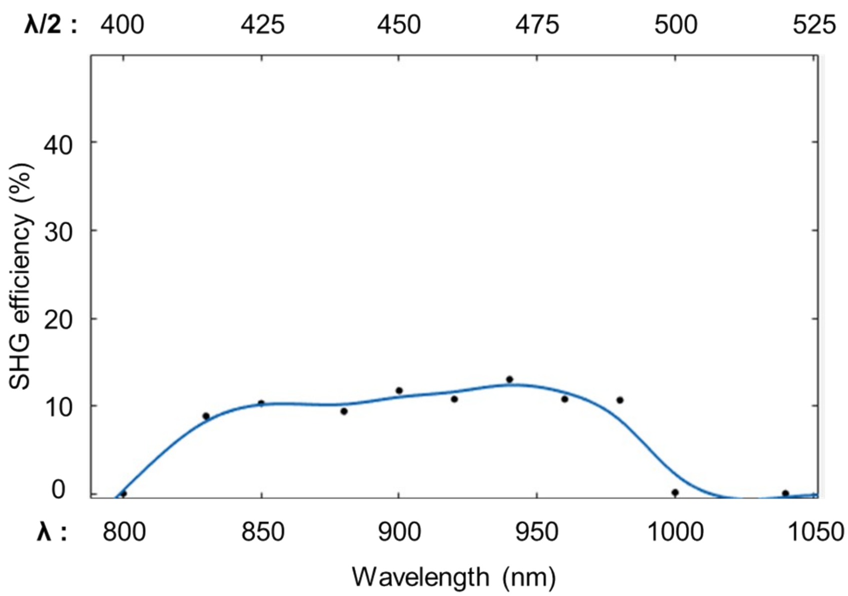

Figure S9: Efficiency of the system components for series of wavelengths.

Table S1 presents an example of the complete calculation for triangle hole array, with a periodicity of 405 nm.

Table S1: Conversion efficiency

Parameter	**SHG emitted photons (CPS)**	**SHG photon energy** (J)	**SHG Power (W)**	**Laser power (average) (W)**	**Conversion efficiency**
Symbol/ Equation	$\frac{N}{\Delta t}$	$E_{ph,\,SHG} = \frac{hc}{\lambda_{SH}}$ *	$\langle P_{SHG}\rangle = \frac{N}{\Delta t} \cdot E_{ph,SHG}$	$\langle P_{FW}\rangle$	$\eta_{SHG} = \frac{\langle P_{SHG}\rangle}{\langle P_{FW}\rangle}$ * *
$P = 455$ nm, triangles hole array, Al (max, Ava 2 ch_s)	307692	4.23×10^{-19}	1.3×10^{-13}	$5\text{x}10^{-3}$	2.6×10^{-11}
$P = 405$ nm,	205754	4.23×10^{-19}	8.7×10^{-14}	$5\text{x}10^{-3}$	$1.74\text{x}10^{-11}$

triangles hole array, Al					
P = 405 nm, triangles hole array, Au	169815	4.23×10^{-19}	7.18×10^{-14}	$8\text{x}10^{-3}$	8.97×10^{-12}
Al surface	770	4.23×10^{-19}	3.3×10^{-16}	$5\text{x}10^{-3}$	6.6×10^{-14}

* For 470 nm, h = 6.63×10^{-34} J·s is Planck's constant, and c = 3×10^{8} m/s is the speed of light in vacuum.

** η is the average conversion efficiency.

Table S2: The effective nonlinear coefficient.

Parameter	**SHG Peak power (W)**	**Laser peak power (W)**	**Peak Nonlinear Coefficient (W^{-1})**
Symbol/ Equation	$\hat{P}_{SHG} = \frac{< P_{SHG} >}{\tau\nu}$ *	$\hat{P}_{FW} = \frac{< P_{FW} >}{\tau\nu}$	$\gamma_{SHG} = \frac{\hat{P}_{SHG}}{(\hat{P}_{FW})^2}$ **
P = 455 nm, triangles hole array, Al (max, Ava 2 ch_s)	1.6×10^{-8}	625	$4.16\text{x}10^{-14}$
P = 405 nm, triangles hole array, Al	$1.08\text{x}10^{-8}$	625	$2.78\text{x}10^{-14}$
P = 405 nm, triangles hole array, Au	8.97×10^{-9}	1000	8.97×10^{-15}
Al surface	6.6×10^{-11}	625	1.6×10^{-19}

* $< P_{SHG} >$ values taken from Table S1.

** γ is the effective nonlinear coefficient.

For each laser pulse, the intensity of the irradiated beam (fundamental, FW) is $\hat{I}_{FW} = \hat{P}_{FW}/(\nu \cdot \tau \cdot A) = 1.51 \cdot 10^{14} W/m^2$, where $\hat{P}_{FW} = \frac{< P_{FW} >}{\tau\nu} = 625\ W$ is the average laser power (tunable), $\nu = 80\ MHz$ is the repetition rate of the laser, $\tau \approx 100\ fs$ is the laser pulse duration, and $A = \pi(r_{FW})^2 = 4.13 \times 10^{-12}\ m^2$ is the measured spot area at the fundamental (λ =

940 nm). $A = \pi(r_{SHG})^2 = 1.03 \times 10^{-12}\, m^2$ is the measured spot area at the focus of the laser (λ = 470 nm).

Table S3: The SHG susceptibility.

Parameter	**Fundamental intensity** $(\frac{W}{m^2})$	**SHG intensity** $(\frac{W}{m^2})$	**Frequency** $(\frac{1}{s})$	**Sample depth (m)**	**SHG susceptibility** $(\frac{pm}{V})$
Symbol/ Equation	$I_{FW} = \frac{2\hat{P}_{FW}}{A_{FW}*}$	$I_{SHG} = \frac{2\hat{P}_{SHG}}{A_{SHG}*}$	$\omega = \frac{2\pi c}{\lambda n}$	L	$\chi_{eff}^{(II)} = \frac{\sqrt{I_{SHG}}}{I_{FW}} \cdot \sqrt{\frac{8\varepsilon_0 c}{2\omega L}}$
P = 455 nm, triangles hole array, Al (max, Ava 2 ch_s)	3.02×10^{14}	3.1×10^4	2×10^{15}	105×10^{-9}	0.06
P = 405 nm, triangles hole array, Al	3.02×10^{14}	2.09×10^4	2×10^{15}	105×10^{-9}	0.05
P = 405 nm, triangles hole array, Au	4.84×10^{14}	1.7×10^4	2×10^{15}	104×10^{-9}	0.028
Al surface	3.02×10^{14}	128	2×10^{15}	105×10^{-9}	0.004

* A_ω , $A_{2\omega}$ values are present before table S3.

$$\varepsilon_0 = 8.85 \times 10^{-12}\left(\frac{F}{m}\right) = 8.85 \times 10^{-12}\left(\frac{Ws}{V^2 m}\right)$$

$$c = 3 \times 10^8\left(\frac{m}{s}\right)$$

The nonlinear coefficient, the fundamental wavelength intensity, and the production rates of SH photons are on the same scale as reported in similar works[1]–[4].

[1] R. Ron, O. Shavit, H. Aharon, M. Zielinski, M. Galanty, and A. Salomon, "Nanoporous Metallic Network as a Large-Scale 3D Source of Second Harmonic Light," *J. Phys. Chem. C*, vol. 123, no. 41, pp. 25331–25340, 2019.

[2] M. Galanty *et al.*, "Second harmonic generation hotspot on a centrosymmetric smooth silver surface," *Light Sci. Appl.*, vol. 7, no. 1, p. 45, 2018.

[3] M. Celebrano *et al.*, "Mode matching in multiresonant plasmonic nanoantennas for enhanced second harmonic generation," *Nat. Nanotechnol.*, vol. 10, no. 5, pp. 412–417, 2015.

[4] J. A. H. Van Nieuwstadt *et al.*, "Strong modification of the nonlinear optical response of metallic subwavelength hole arrays," *Phys. Rev. Lett.*, vol. 97, no. 14, pp. 1–4, 2006.